Scattering by Thin Wires and Finite Rectangular Grooves Using a Physical Basis Model

Authors: Arindam Chatterjee and John L. Volakis

January 1991

SCATTERING BY THIN WIRES AND FINITE RECTANGULAR GROOVES USING A PHYSICAL BASIS MODEL

Arindam Chatterjee and John L. Volakis
Radiation Laboratory
Department of Electrical Engineering and Computer Science
University of Michigan
Ann Arbor, MI 48109-2122

Abstract

The problem of scattering and diffraction by thin wires has been investigated by many authors primarily because the wire is one of the very few practical geometries amenable to an analytic solution. Similar analyses, though, for the coated wire or related geometries such as the finite length narrow groove have not been considered. In this paper, we employ the travelling wave model in conjunction with a Galerkin's solution of the exact integral equation to solve for the scattering by a thin perfectly conducting wire, a thin dielectrically coated wire and a finite length narrow groove in a ground plane. As usual, the proposed current model consists of three weighted travelling wave components; one is associated with the current on the finite wire whereas the other two describe the reflected travelling waves from the wire terminations. For the coated wire, their coefficients are evaluated analytically through a convenient variable transformation. In the case of the finite length narrow groove, an approximate impedance boundary condition is employed at the surface of the groove for constructing the integral equation involving a surface magnetic current which is then represented by the weighted sum of the three travelling wave components. The associated travelling wave coefficients are found in terms of single integrals which are reduced from the original quadruple integrals by employing certain variable transformations. Several current distributions and scattering patterns are presented which serve to validate the accuracy of the model and the derived analytical formulae.

1 Introduction

The problem of scattering and diffraction by thin wires has been investigated by many authors [1-19] primarily because the wire is one of the very few practical geometries amenable to an analytic solution. The cited references are a representative subset of the numerous works on the subject and based on the approach of analysis, these can be generally cast into three categories. In [1](method A), [2] and [3], the wire current is postulated within some constants which are then determined by the application of conservation of energy or a variational approach. The resulting solutions, although lengthy, are in terms of the exponential integrals. However, due to the approximations required in the process, the solution for long wires given by Van Vleck, etc. fails for near grazing incidences whereas that of Tai [2] fails in the vicinity of normal incidence.

The solutions presented in [4-11] and [1] (method B) are based on an iterative or some approximate [9-11] solution of the associated integral equation for the wire current and have been quoted to be primarily restricted to small wire lenghts. A third class of solutions [12-17] are based on a travelling wave model [18] for the wire current in conjunction with the Wiener-Hopf solution [19] for the semi-infinite wire. The resulting current expressions are generally cumbersome but more accurate than those based on other approaches. Chen [20] also employed the Wiener-Hopf technique to arrive at an expression for the wire current with plane wave illumination (see also Wu[21] for normal incidence) but due to the approximations included in his derivation, the given results are only applicable for long wires. In contrast, those based on the travelling wave model are suited for wire lengths from a small fraction of a wavelength and up.

In this work, we employ the travelling wave model in conjunction with a Galerkin's solution of the exact integral equation to solve for the scattering by a thin perfectly conducting wire, a thin dielectrically coated wire and a finite length narrow groove in a ground plane. As usual, the proposed current model consists of three weighted travelling wave components which will be referred to as the physical basis of the expansion. One is associated with the current on the finite wire whereas the other two describe the reflected travelling waves from the wire terminations. Their coefficients are rigorously determined by constructing a 3×3 matrix through a Galerkin's discretization of the pertinent integral equation. In the case of the perfectly conducting

wire, the impedance matrix elements are evaluated analytically through a variable transformation employed by Richmond [22] in connection with his analysis of the dielectric strip. For the finite length narrow groove, an approximate impedance boundary condition [23] is employed at the surface of the groove for constructing the integral equation involving a surface magnetic current which is then represented by the weighted sum of the aforementioned three travelling wave components. Galerkin's technique is again employed for the discretization of the integral equation. However, in this case, the same variable transformation used for the evaluation of the impedance element in connection with the wire allows only a reduction of the quadruple to single integrals, which are then computed numerically.

The presented formulation and scattered field expressions for the coated wire are, of course, new since all of the above references have dealt with the perfectly conducting wire and the same holds for the finite length narrow groove. However, our solution for the perfectly conducting wire should also be found useful and less cumbersome than others in the literature. In the next section, we first present the solution for the perfectly conducting wire followed by the analysis of the coated wire and that of the finite length narrow groove. Several computations are then included and discussed for the wires and finite length groove. These serve to assess the validity of the model and the accuracy of the derived analytical expressions.

2 Perfectly conducting wire

Consider the thin straight wire illustrated in figure 1 of radius a and length $2l$. Assuming the wire is illuminated by the plane wave (an $e^{j\omega t}$ time dependence is assumed and suppressed)

$$\begin{aligned} \mathbf{E}^{\mathrm{i}} &= \hat{\theta}_o E_o e^{jk_o\{z\cos\theta_o + x\sin\theta_o\}} \\ &= (\hat{x}\cos\theta_o\cos\phi_o + \hat{y}\cos\theta_o\sin\phi_o - \hat{z}\sin\theta_o) E_o e^{jk_o(x\sin\theta_o + z\cos\theta_o)} \end{aligned} \quad (1)$$

where $k_o = 2\pi/\lambda$ is the free space propagation constant, a surface current will be generated on the wire and we are interested in an analytic evaluation of this current. Provided $a \ll \lambda$ and $2l/a \gg 1$, the wire surface current may be replaced by a z-directed filamentary current at its center (see Fig. 1). For an infinite wire, this current is expected to have the same z-dependence

as the incident field and can thus be expressed as

$$I(z) = I_0(z) \;=\; Ce^{jk_o z\cos\theta_o}$$

where C is an attachment constant. By terminating the infinite wire, additional current components are generated due to the reflection of $I_0(z)$ at the wire terminations and on the assumption that the reflected currents propagate with the free space velocity, an appropriate representation for the total current on the finite wire is

$$\begin{aligned} I(z) &= C_1 e^{jk_o z} + C_2 e^{-jk_o z} + C_3 e^{jk_o z cos\theta_o} \\ &= \sum_{n=1}^{3} C_n B_n(z) \end{aligned} \tag{2}$$

In this, C_n are constants to be determined by enforcing the required boundary conditions and $B_n(z)$ can be referred to as the physical expansion basis. The Fourier transform of the current to be denoted as $\widetilde{I(k_z)}$ is readily found to be

$$\begin{aligned} \widetilde{I(k_z)} &= \mathcal{F}\{I(z)\} \\ &= 2l\left\{C_1 sinc[(k_z - k_o)l] + C_2 sinc[(k_z + k_o)l] + C_3 sinc[(k_z - k_o\cos\theta_o)l]\right\} \end{aligned}$$

where $sinc(x) = sin(x)/x$ and the current spectrum is seen to be a sum of three sinc functions shifted from zero by an amount proportional to the propagation constant of the associated current components. Thus one can readily test the validity of the model by comparing $\widetilde{I(k_z)}$ with the wire current spectra obtained from a direct moment method solution of Pocklington's integral equation. For example, figure 2 displays the current spectrum of a 4λ wire illuminated at $\theta_o = 60^o$ and 90^o and these are seen to agree with the proposed model. Comparisons with current spectra for shorter and longer wires also resulted in similar conclusions.

To determine the constants C_n, we now refer to Pocklington's integral equation,

$$E_z^i(x = a, z) \;=\; jk_o Z_o \int_{-l}^{l} I(z') \left[1 + \frac{1}{k_o^2}\frac{d^2}{dz^2}\right] \frac{e^{-jk_o R}}{4\pi R} dz' \tag{3}$$

where

$$R = \sqrt{(z-z')^2 + a^2}$$

and Z_o is the free space intrinsic impedance. Substituting (2) into (3) yields

$$E_z^i(x=a,z) \;=\; jk_oZ_o \int_{-l}^{l} \sum_{n=1}^{3} C_n B_n(z') \left[1 + \frac{1}{k_o^2}\frac{d^2}{dz^2}\right] \frac{e^{-jk_oR}}{4\pi R} dz', \qquad (4)$$

and upon employing Galerkin's procedure, we obtain the 3×3 matrix system

$$[Z_{mn}][C_n] = [V_m] \qquad (5)$$

for a solution of the three constants C_n. In the above ,

$$\begin{aligned} V_m &= \int_{-l}^{l} E_z^{inc}(x=a,z) B_m^*(z) dz \\ &= -2E_{\theta_o}\, l\, sin\theta_o \frac{sin[k_o(cos\theta_o - p_m)l]}{k_o(cos\theta_o - p_m)} \qquad (6) \\ Z_{mn} &= j\frac{Z_o}{k_o}\frac{k_o^2 - p_n^2}{4\pi} \int_{-l}^{l}\int_{-l}^{l} B_n(z') B_m^*(z) \frac{e^{-jk_oR}}{R} dz\, dz' \\ &= j\frac{Z_o}{k_o}\frac{k_o^2 - p_n^2}{4\pi} \int_{-l}^{l}\int_{-l}^{l} e^{-jk_o(p_m z - p_n z')} \frac{e^{-jk_oR}}{R} dz\, dz' \\ &= j\frac{Z_o}{k_o}\frac{k_o^2 - p_n^2}{4\pi} \widetilde{Z_{mn}} \qquad (7) \end{aligned}$$

in which $p_1 = k_o$, $p_2 = -k_o$ and $p_3 = k_o cos\theta$ denote the propagation constants of the three travelling waves. Given the constants C_n, the scattered far-field is readily found to be

$$\begin{aligned} E_\theta^r &= -jk_oZ_o\, sin\theta \frac{e^{-jk_or}}{4\pi r} \int_{-l}^{l} I(z') e^{jk_oz'\, cos\theta} dz' \\ &= -2jk_oZ_o\, l\, sin\theta \frac{e^{-jk_or}}{4\pi r} \sum_{n=1}^{3} C_n sinc[(k_o cos\theta + p_n)l] \qquad (8) \end{aligned}$$

To evaluate the double integral $\widetilde{Z_{mn}}$, we resort to the variable transformation [22]

$$\begin{aligned} z &= (u-v)/\sqrt{2} \\ z' &= (u+v)/\sqrt{2} \qquad (9) \end{aligned}$$

which allows us to express R in terms of a single variable. In particular, by making use of (9) in (7), we have

$$\widetilde{Z_{mn}} = \int_{-l'}^{l'} \left(\int_{-u_2}^{u_2} e^{-jk_o(\frac{p_m - p_n}{\sqrt{2}})u} \, du \right) e^{jk_o \frac{p_m + p_n}{\sqrt{2}} v} \, \frac{e^{-jk_o R}}{R} \, dv \qquad (10)$$

where $l' = \sqrt{2}l$, $u_2 = l' - |v|$, and $R = \sqrt{2v^2 + a^2}$. Integrating now with respect to u yields

$$\begin{aligned} \widetilde{Z_{mn}} &= \frac{4\sqrt{2}}{k_o(p_m - p_n)} \int_0^{l'} sin\left[\frac{k_o(p_m - p_n)(l' - v)}{\sqrt{2}}\right] cos\left[\frac{k_o(p_m + p_n)v}{\sqrt{2}}\right] \frac{e^{-jk_o R}}{R} \, dv \\ &= \int_0^{l'} K(v) dv \end{aligned}$$

where we have assumed that $m \neq n$. To permit an analytical evaluation of $\widetilde{Z_{mn}}$, we break up the above integral as

$$\begin{aligned} \widetilde{Z_{mn}} &= \widetilde{Z^1_{mn}} + \widetilde{Z^2_{mn}} \\ &= \int_0^{v_1} K(v) dv + \int_{v_1}^{l'} K(v) dv \end{aligned} \qquad (11)$$

where v_1 is chosen to be a small positive number (for example, $\sqrt{2}k_o v_1 = 3$) so that the approximation

$$\frac{e^{-jk_o R}}{R} = \frac{1}{R} - jk_o \qquad (12)$$

can be introduced in the integrand of $\widetilde{Z^1_{mn}}$. Doing so yields

$$\begin{aligned} \widetilde{Z^1_{mn}} &= \frac{2\sqrt{2}}{k_o(p_m - p_n)} \int_0^{v_1} \left\{ sin[k_1 + \sqrt{2}k_o p_n v] + sin[k_1 - \sqrt{2}k_o p_m v] \right\} \left[\frac{1}{R} - jk_o \right] dv \\ &= \frac{2\sqrt{2}}{k_o(p_m - p_n)} \left[\int_0^{v_1} \frac{sin[k_1 + \sqrt{2}k_o p_n v]}{R} dv + \int_0^{v_1} \frac{sin[k_1 - \sqrt{2}k_o p_m v]}{R} dv \right. \\ &\quad \left. -jk_o \left\{ \int_0^{v_1} sin[k_1 + \sqrt{2}k_o p_n v] dv + \int_0^{v_1} sin[k_1 - \sqrt{2}k_o p_m v] dv \right\} \right] \end{aligned}$$

and by carrying out the integrations and simplifying, we find

$$\widetilde{Z^1_{mn}} = \frac{2\sqrt{2}}{k_o(p_m - p_n)} \left[\widetilde{Z^{1a}_{mn}} + \widetilde{Z^{1b}_{mn}} + \widetilde{Z^{1c}_{mn}} + \widetilde{Z^{1d}_{mn}} \right], m \neq n \qquad (13)$$

where

$$k_1 = k_0 \frac{(p_m - p_n)}{\sqrt{2}} l'$$

$$\begin{aligned}
\widetilde{Z_{mn}^{1a}} &= \frac{\sin A}{\sqrt{2}} \left[\left\{ (1 + \frac{t_1^2}{4}) \, sinh^{-1} \left(\frac{s_1}{t_1} \right) - \frac{s_1}{4} \sqrt{s_1^2 + t_1^2} \right\} \Big|_{s_1=0}^{s_1=\sqrt{2}kp_n v_1} \right. \\
&\quad \left. + \left\{ (1 + \frac{t_2^2}{4}) \, sinh^{-1} \left(\frac{s_2}{t_2} \right) - \frac{s_2}{4} \sqrt{s_2^2 + t_2^2} \right\} \Big|_{s_2=0}^{s_2=\sqrt{2}kp_m v_1} \right] \\
\widetilde{Z_{mn}^{1b}} &= \frac{\cos A}{\sqrt{2}} \left\{ \sqrt{s_1^2 + t_1^2} \left[1 - \frac{1}{18} \left(s_1^2 - 2t_1^2 \right) \right] \right\} \Big|_{s_1=0}^{s_1=\sqrt{2}kp_n v_1} \\
&\quad - \frac{\cos A}{\sqrt{2}} \left\{ \sqrt{s_2^2 + t_2^2} \left[1 - \frac{1}{18} \left(s_2^2 - 2t_2^2 \right) \right] \right\} \Big|_{s_2=0}^{s_2=\sqrt{2}kp_m v_1} \\
\widetilde{Z_{mn}^{1c}} &= \frac{j}{2\sqrt{2}} \frac{1}{p_n} \left\{ cos(A + \sqrt{2}kp_n v_1) - cos \, A \right\} \\
\widetilde{Z_{mn}^{1d}} &= -\frac{j}{2\sqrt{2}} \frac{1}{p_m} \left\{ cos(A - \sqrt{2}kp_m v_1) - cos \, A \right\}
\end{aligned}$$

in which $A = k(p_m - p_n)l$, $t_1 = kp_n a$ and $t_2 = kp_m a$.

To evaluate $\widetilde{Z_{mn}^2}$, we set

$$R = \sqrt{2v^2 + a^2} \approx \sqrt{2}v$$

in the integrand since $v \gg a$. Substituting this into (11) yields

$$\begin{aligned}
\widetilde{Z_{mn}^2} &= \frac{1}{jk_o(p_m - p_n)} \left[e^f \left\{ \int_{v_1}^{l'} \frac{e^{j\sqrt{2}k_o(p_n - 1)v}}{v} dv + \int_{v_1}^{l'} \frac{e^{-j\sqrt{2}k_o(p_m + 1)v}}{v} dv \right\} \right. \\
&\quad \left. - e^{-f} \left\{ \int_{v_1}^{l'} \frac{e^{j\sqrt{2}k_o(p_m - 1)v}}{v} dv + \int_{v_1}^{l'} \frac{e^{-j\sqrt{2}k_o(p_n + 1)v}}{v} dv \right\} \right] \\
&= \frac{1}{jk_o(p_m - p_n)} \left[e^f (\widetilde{Z_{mn}^{2a}} + \widetilde{Z_{mn}^{2b}}) - e^{-f} (\widetilde{Z_{mn}^{1c}} + \widetilde{Z_{mn}^{1d}}) \right], m \neq n \qquad (14)
\end{aligned}$$

where

$$
\begin{aligned}
f &= jk_o\frac{(p_m-p_n)}{\sqrt{2}}l' \\
\widetilde{Z^{2a}_{mn}} &= E_+(\sqrt{2}k_o(p_n-1)) \\
\widetilde{Z^{2b}_{mn}} &= E_-(\sqrt{2}k_o(p_m+1)) \\
\widetilde{Z^{2c}_{mn}} &= E_+(\sqrt{2}k_o(p_m-1)) \\
\widetilde{Z^{2d}_{mn}} &= E_-(\sqrt{2}k_o(p_n+1))
\end{aligned}
$$

and

$$
E_{\pm}(x) = Ci(l'x)\overset{+}{-}j\ si(l'x) - Ci(v_1x)\overset{-}{+}j\ si(v_1x)
$$

in which

$$
si(x) = -\int_x^\infty \frac{sin\,t}{t}dt, \quad Ci(x) = -\int_x^\infty \frac{cos\,t}{t}dt
$$

denote the sine and the cosine integrals, respectively.

To obtain the corresponding analytical expressions for the diagonal impedance elements Z_{mm}, we return to (10). By integrating with respect to u, we obtain

$$
\begin{aligned}
\widetilde{Z_{mm}} &= 4\int_0^{l'}(l'-v)cos(\sqrt{2}kp_mv)\frac{e^{-jk\sqrt{2v^2+a^2}}}{\sqrt{2v^2+a^2}}dv \\
&= 4\left[\int_0^{v_1}(l'-v)cos(\sqrt{2}kp_mv)\frac{e^{-jk\sqrt{2v^2+a^2}}}{\sqrt{2v^2+a^2}}dv + \int_{v_1}^{l'}(l'-v)cos(\sqrt{2}kp_mv)\frac{e^{-jk\sqrt{2v^2+a^2}}}{\sqrt{2v^2+a^2}}dv\right]
\end{aligned}
\tag{15}
$$

and as before this can be written as

$$
\widetilde{Z_{mm}} = 4\,(\widetilde{Z^1_{mm}} + \widetilde{Z^2_{mm}})
$$

Following a procedure similar to that employed above, we find

$$
\begin{aligned}
\widetilde{Z^1_{mm}} &= l\left\{\left[(1+\frac{t_1^2}{4})\,sinh^{-1}\left(\frac{s_1}{t_1}\right) - \frac{s_1}{4}\sqrt{s_1^2+t_1^2}\right]\right. \\
&\quad \left.-\frac{1}{\sqrt{2}k}\sqrt{s_1^2+t_1^2}\left[1-\frac{1}{6}\left(s_1^2-2t_1^2\right)\right]\right\}\Bigg|_{s_1=0}^{s_1=\sqrt{2}kp_mv_1} \\
&\quad -jlsin(\sqrt{2}kp_mv_1) + \frac{j}{\sqrt{2}}\left[v\ sin(\sqrt{2}kp_mv) + \frac{cos(\sqrt{2}kp_mv)}{\sqrt{2}k}\right]\Bigg|_{v=0}^{v=v_1}
\end{aligned}
\tag{16}
$$

where $t_1 = kp_m a$. In addition, $\widetilde{Z^2_{mm}}$ is given by (14) upon setting $m = n$.

This completes the derivation of all impedance matrix elements. The coefficients of the travelling wave components can now be readily evaluated from (5) by inverting the 3×3 impedance matrix.

3 Coated Wire

Let us now consider the scattering by a thin dielectrically coated wire. As illustrated in figure 3, a uniform coating of thickness $(b-a)$ is placed over a perfectly conducting wire of radius a. We shall assume that $ka \ll 1$, $kb \ll 1$ with a and b also much smaller than the wire length.

When the coated wire is subjected to a field excitation $\mathbf{E^i}$, there will be polarization currents due to the presence of the coating, in addition to the filamentary current $I(z)$ through the perfect conductor. By invoking the equivalence principle, the polarization currents can be expressed as

$$\mathbf{J} = \hat{\rho} j k_o Y_o (\epsilon_r - 1) E_\rho \tag{17}$$

for $a < \rho < b$, where (ρ, ϕ) denote the usual cylindrical coordinates and $Y_o = 1/Z_o$ is the free space admittance. In addition, ϵ_r is the relative permittivity of the coating and we have assumed $E_z \approx 0$ since $k_o(b-a) \ll 1$. From Maxwell's equations [24], the radiated field due to the electric current density (17) is identical to that generated by the magnetic current

$$M_\phi = -\frac{jZ_o}{k_o}\left(\hat{\phi} \cdot \nabla \times \mathbf{J}\right) = (\epsilon_r - 1)\frac{\partial E_\rho}{\partial z} = -\left(\frac{\epsilon_r - 1}{j k_o Y_o \epsilon_r}\right)\frac{\partial^2 H_\phi}{\partial z^2} \tag{18}$$

Based on symmetry, H_ϕ is not a function of ϕ, and thus from Ampere's law we obtain

$$M_\phi = -\left(\frac{\epsilon_r - 1}{j k_o Y_o \epsilon_r}\right)\frac{1}{2\pi\rho}\frac{\partial^2 I(z)}{\partial z^2} \tag{19}$$

which is a relation between the filamentary current through the conductor and the polarization current in the dielectric.

The magnetic current density defined in (19) is uniformly distributed over $a < \rho < b$ and it is convenient to replace it by a current sheet at $\rho = (a+b)/2$ supporting the surface current (see Figure 3)

$$M_{s\phi} = \int_a^b M_\phi(\rho)d\rho$$
$$= -\left(\frac{\epsilon_r - 1}{jk_oY_o\epsilon_r}\right)\ln\left(\frac{b}{a}\right)\frac{\partial^2 I}{\partial z^2}$$

Subsequently by invoking the sheet boundary condition, $\mathbf{M} = \mathbf{E} \times \hat{\rho}$, we have

$$E_z = -\left(\frac{\epsilon_r - 1}{jk_oY_o\epsilon_r}\right)\ln\left(\frac{b}{a}\right)\frac{\partial^2 I}{\partial z^2} \tag{20}$$

which is an approximate relation to be enforced at $\rho = (a+b)/2$ instead of $E_z = 0$ applicable to the uncoated wire. One may also consider (20) as an approximation of the scattered field attributed to the polarization currents in the coating.

As in the previous section, in order to derive an integral equation for $I(z)$, we adopt the physical basis representation (3) and proceed with the enforcement of (20). In this case, however, p_1 and p_2 are not equal to k_o and must be computed by an iterative solution of the transcendental equation given in the Appendix. Following Galerkin's method, we obtain

$$\int_{-l/2}^{l/2} E_z^i(z)B_m^*(z)dz = -\int_{-l/2}^{l/2} E_z^s(z)B_m^*(z)dz + \sum_{n=1}^{3} C_n\left(\frac{Z'_{s_{mn}}}{2\pi a}\right)\int_{l/2}^{l/2} B_n(z)B_m^*(z)dz \tag{21}$$

where E_z^s is the z-component of the scattered field and is equal to the negative of the right-hand side of (5). Also,

$$Z'_{s_{mn}} = -\frac{p_n p_m(\epsilon_r - 1)}{jk_oY_o\epsilon_r} a\ln\left(\frac{b}{a}\right)$$

which resulted after integrating by parts the last integral in (21) . It should be noted, though, that were we to consider the solution for a thin wire having a surface impedance Z_s [25], the resulting integral equation is again (21) with Z'_{smn} replaced by Z_s. Interestingly, since $Z'_{s_{mn}}$ is not zero for $n \neq m$, we cannot identify a constant equivalent impedance to replace the coating. From (21), the resulting matrix equations for a solution of the travelling wave coefficients can be written as

$$[Z'_{mn}][C_n] = [V_m] \tag{22}$$

In this case, V_m is again given by (6) and

$$Z'_{mn} = Z_{mn} + \frac{Z'_{s_{mn}}}{2\pi a} sinc\left(\frac{p_n - p_m}{2} l\right)$$

where Z_{mn} are given by (7) as one can readily conclude from a comparison of (21) and (7).

4 Finite length narrow rectangular groove

In this section, we consider an empty three dimensional rectangular cavity of width $2w \ll \lambda$ and length $2l \gg \lambda$ (see Figure 4). The opening of the cavity lies in an infinite ground plane and we are interested in its scattering characteristics when illuminated by a plane wave . The incident electric field may be expressed as

$$\mathbf{E^i} = (\hat{\theta}_o E^i_{\theta_o} + \hat{\phi}_o E^i_{\phi_o})\, e^{-j\bar{k}_i.\bar{r}} \tag{23}$$

and in the absence of a cavity, the incident plane wave (23) will only cause a reflected field $\mathbf{E^r}$.

An approximate simulation of the cavity is to replace its aperture by an impedance surface on the ground plane satisfying the boundary conditions

$$\begin{aligned} E_x &= -Z_o \eta_h H_y \\ E_y &= Z_o \eta_e H_x \end{aligned} \tag{24}$$

where $\eta_{e,h}$ are the normalized impedance parameters given by [23]

$$\begin{aligned} \eta_h &= j\frac{\alpha_h}{\epsilon_r} tan(\alpha_h k_o d) \\ \eta_e &= j\frac{\mu_r}{\alpha_e} tanh(\alpha_e k_o d) \end{aligned}$$

in which

$$\begin{aligned} \alpha_h &= \sqrt{\epsilon_r \mu_r} \\ \alpha_e &= \sqrt{\left(\frac{\lambda}{2w}\right)^2 - \epsilon_r \mu_r} \end{aligned}$$

and d denotes the cavity depth. As can be readily concluded, (24) were derived on the assumption that only the lowest order TE and TM modes exist in the groove.

By invoking the equivalence principle, the electric field in (24) can be replaced by the equivalent surface magnetic current

$$\mathbf{M} = \mathbf{E} \times \hat{z} \tag{25}$$

and from (25), we obtain

$$\begin{aligned} M_x &= Z_o \eta_e H_x \\ M_y &= Z_o \eta_h H_y \end{aligned} \tag{26}$$

in which $H_{x,y}$ denote the x and y components of the total magnetic field. This can be represented as

$$\mathbf{H} = \mathbf{H^i} + \mathbf{H^r} + \mathbf{H^s} \tag{27}$$

where $\mathbf{H^i}$ is the incident field, $\mathbf{H^r}$ is the reflected field in the absence of the cavity and $\mathbf{H^s}$ denotes the scattered field radiated by M_x and M_y. Since only long and narrow geometries are considered, the transverse component of the magnetic current can be neglected and the longitudinal component of the current may be assumed to be constant across the width of the groove. Consequently, we can express the y component of the scattered field as

$$H_y^s = -2j\frac{Y_o}{k_o}\int_{-w}^{w}\int_{-l}^{l} M_y(y')(k_o^2 + \frac{\partial^2}{\partial y^2})G_o(x,x',y,y')dx'dy' \tag{28}$$

where

$$G_o(x,x'y,y') = \frac{exp(-jk_o\sqrt{(x-x')^2+(y-y')^2})}{4\pi\sqrt{(x-x')^2+(y-y')^2}}$$

is the free-space Green's function. Combining (26),(27) and (28), we obtain

$$\frac{1}{2\eta_h}M_y = I_y^i - \frac{j}{k_o}\int_{-w}^{w}\int_{-l}^{l} M_y(y')(k_o^2 + \frac{\partial^2}{\partial y^2})G_o(x,x',y,y')dx'dy' \tag{29}$$

to be solved for M_y, where

$$\begin{aligned} I_y^i &= Z_o(H_y^i + H_y^r)\Big|_{z=0} \\ &= 2\left[-cos\phi_o E_{\theta_o}^o + cos\theta_o sin\phi_o E_{\phi_o}^i\right] e^{jk_o(xcos\phi_o sin\theta_o + ysin\phi_o sin\theta_o)} \end{aligned} \tag{30}$$

As in the case with the wire, $M_y(y)$ can be represented by three travelling wave components for depths greater than $\lambda/4$. For troughs of depth less than $\lambda/4$, though, the reflected travelling wave currents diminish leaving a single dominant travelling wave component. This is evident from the spectral plots of $M_y(y)$ in figure 5 obtained from the finite-element code described in [26]. Included in figure 5 are the spectra for a 5λ long groove of width $.05\lambda$ and it is clear that the surface current for the cavity of depth $.1\lambda$ is associated only with the forced travelling wave component. In contrast, for the $.4\lambda$ deep cavity, the forced component is nearly suppressed whereas the reflected travelling waves are dominant. Accordingly, an appropriate representation for the surface magnetic current is

$$\begin{aligned} M_y(y) &= C_1 e^{\gamma y} + C_2 e^{-\gamma y} + C_3 e^{jk_o y sin\theta sin\phi} \\ &= \sum_{n=1}^{3} C_n D_n(y) \end{aligned} \tag{31}$$

where $\gamma = -\alpha + j\beta$ can be calculated from Walter's formula [27] and the procedure outlined in [28]. Substituting (31) into (29) and using Galerkin's technique results in the 3×3 matrix system

$$[Y_{mn}][C_n] = [I_m] \tag{32}$$

for the solution of the coefficients C_n. In this

$$\begin{aligned} I_m &= \int_{-l}^{l}\int_{-w}^{w} I_y^i D_m^*(y) dx\, dy \\ &= 8wl\left[-cos\phi_o E_{\theta_o}^o + cos\theta_o sin\phi_o E_{\phi_o}^i\right] sinc\left(k_o w\, cos\phi_o sin\theta_o\right) sinc\left((k_o sin\phi_o sin\theta_o - p_m^*)l\right) \\ Y_{mn} &= \frac{1}{2\eta_h}\int_{-l}^{l}\int_{-w}^{w} D_n(y) D_m^*(y) dx\, dy \\ &\quad + \frac{j(k_o^2 - p_n^2)}{k_o}\int_{-l}^{l}\int_{-l}^{l}\int_{-w}^{w}\int_{-w}^{w} D_n(y') D_m^*(y) G_o(x, x', y, y') dx dx' dy dy' \\ &= \frac{2wl}{\eta_h} sinc\left((p_n - p_m^*)l\right) + \frac{j(k_o^2 - p_n^2)}{k_o}\widetilde{Y_{mn}} \end{aligned}$$

where $p_1 = -\alpha + j\beta$, $p_2 = \alpha - j\beta$ and $p_3 = jk_o \sin\theta_o \sin\phi_o$ denote the propagation constants for the travelling wave components and

$$\widetilde{Y_{mn}} = \int_{-l}^{l}\int_{-l}^{l}\int_{-w}^{w}\int_{-w}^{w} e^{-j(p_m^* y - p_n y')} G_o(x, x', y, y') dx dx' dy dy'$$

As before, on carrying out the variable transformation [22] corresponding to a 45° coordinate rotation, the above quadruple integral for $\widetilde{Y_{mn}}$ reduces to a double integral. Specifically, we have

$$\widetilde{Y_{mn}} = \frac{16}{p_m^* - p_n} \int_0^{l'} \int_0^{w'} sin\left[\frac{(p_m^* - p_n)(l'-v)}{\sqrt{2}}\right] cos\left[\frac{(p_m^* + p_n)v}{\sqrt{2}}\right] \left[(w'-t)\frac{e^{-jk_oR}}{R}\, dt\right] dv \tag{33}$$

where $l' = \sqrt{2}l$, $w' = \sqrt{2}w$ and $R = \sqrt{2(t^2+v^2)}$. Further rearrangement then yields

$$\begin{aligned}\widetilde{Y_{mn}} &= \frac{16}{p_m^* - p_n}\left[\int_0^{v_1}\left(\int_0^{w'} K(t,v)dt\right)L(v)dv + \int_{v_1}^{l'}\left(\int_0^{w'} K(t,v)dt\right)L(v)dv\right] \\ &= \frac{16}{p_m^* - p_n}\left(\widetilde{Y_{mn}^1} + \widetilde{Y_{mn}^2}\right) \end{aligned} \tag{34}$$

where

$$\begin{aligned} K(t,v) &= (w'-t)\frac{e^{-jk_oR}}{R} \\ L(v) &= sin\left[\frac{(p_m^* - p_n)(l'-v)}{\sqrt{2}}\right] cos\left[\frac{(p_m^* + p_n)v}{\sqrt{2}}\right] \\ \sqrt{2}k_o v_1 &\simeq 1.4 \end{aligned}$$

The integral $\int_0^{w'} K(t,v)dt$ can be evaluated analytically by expanding e^{-jk_oR}/R in a Taylor series. We have,

$$K(w',v) = \int_0^{w'} (w'-t)\frac{\sum_{a=0}^{b}(-j\sqrt{2}k_oR)^a}{R}\, dt \tag{35}$$

where b denotes the number of terms in the expansion and determines the maximum width of the groove for which the echo-area can be evaluated reliably. On substituting (35) into (34), $\widetilde{Y_{mn}^1}$ reduces to the single integral

$$\widetilde{Y_{mn}^1} = \int_0^{v_1} K(w',v) sin\left[\frac{(p_m^* - p_n)(l'-v)}{\sqrt{2}}\right] cos\left[\frac{(p_m^* + p_n)v}{\sqrt{2}}\right] dv \tag{36}$$

which can be computed numerically. The corresponding integral for $\widetilde{Y_{mn}^2}$ can be simplified using the approximation

$$R = \sqrt{2(v^2+t^2)} \approx \sqrt{2}v \quad \text{for } v \gg t$$

since $v_1 \gg w$, consistent with our assumption of a narrow groove. Consequently,

$$K(w',v) = \int_0^{w'} (w'-t)\frac{e^{-j\sqrt{2}k_o v}}{v}dt = \frac{w'^2}{2}\frac{e^{-j\sqrt{2}k_o v}}{v}$$

and

$$\widetilde{Y^2_{mn}} = \frac{w'^2}{8j}\left[e^F\left\{\int_{v_1}^{l'}\frac{e^{j\sqrt{2}(p_n-k_o)v}}{v}dv + \int_{v_1}^{l'}\frac{e^{-j\sqrt{2}(p_m^*+k_o)v}}{v}dv\right\}\right.$$
$$\left. -e^{-F}\left\{\int_{v_1}^{l'}\frac{e^{j\sqrt{2}(p_m^*-k_o)v}}{v}dv + \int_{v_1}^{l'}\frac{e^{-j\sqrt{2}(p_n+k_o)v}}{v}dv\right\}\right] \quad (37)$$

in which $F = j\frac{(p_m^*-p_n)}{\sqrt{2}}l'$. Clearly, the integrands in the above expression for $\widetilde{Y^2_{mn}}$ are non-singular and therefore the integrals can be readily evaluated numerically.

Given the admittance matrix elements, the 3×3 system (32) can then be solved via a QR decomposition for the constants C_n. Results based on this solution are discussed in the next section along with results for the wire solution.

5 Results

The physical basis model for the wire was studied extensively owing to the wealth of available data. The model was tested for short as well as long wires and was found to predict accurate results in both cases. In all cases, the reference numerical results for the wire are based on a conjugate gradient-FFT (CGFFT) or a moment method solution of Pocklington's integral equation, using a piecewise sinusoidal representation for the current.

Figure 6 shows a comparison of the current distribution for a 4λ wire at normal and oblique ($\theta_o = 60^o$) incidence. As seen the numerical result and that based on the proposed physical basis model are in good agreement. A plot of the physical basis coefficients is given in Figure 7 and it reveals that the magnitude of the travelling wave lobe is governed solely by the corresponding coefficient. The other two coefficients at this angle are equal and opposite in sign, cancelling each other's contribution. At normal incidence, however,

all three coefficients are comparable in value and interfere constructively to produce a peak.

Figure 8 presents backscatter patterns for $\lambda/4$ and 1λ long wires. As seen, the physical basis solution of Pocklington's integral equation is in good agreement with the reference data for both wires and for all angles of incidence. Backscatter patterns for longer wires are given in figures 9 and 10. These correspond to wires of length 3λ and 11.05λ, respectively, and it is again seen that the physical basis solution is in good agreement with the reference data. In the case of the coated wire, two bistatic patterns are given in figure 11. Again, the physical basis solution is in good agreement with the moment method data. It should be noted though that the propagation constant of the reflected travelling wave may now be greater than k_o and as a result, their corresponding peaks are not necessarily in the visible range.

Finally in figure 14, we present the backscatter patterns for a 5λ long cavity. Two patterns are given, one corresponding to a cavity of depth 0.1λ and width 0.05λ and another for a cavity of depth 0.3λ having the same width. The existence of the travelling wave lobe is quite evident for the deeper cavity whereas the scattering pattern for the shallow cavity resembles that of a physical optics approximation. For both patterns, the agreement with the reference data is reasonable and any discrepancy is likely due to the employed impedance boundary condition.

6 Summary

In this work, the physical basis model was employed in conjunction with a Galerkin's solution of the exact integral equation to determine the scattering by a thin perfectly conducting wire, a thin dielectrically coated wire and a finite length narrow groove in a ground plane. The proposed current model consisted of three weighted travelling wave components. One was associated with the current on the finite wire whereas the other two described the reflected travelling waves from the wire terminations. Their coefficients were rigorously determined by constructing a 3×3 matrix through a Galerkin's discretization of the pertinent integral equation. The resulting impedance elements for the perfectly conducting and the coated wire were analytically derived in terms of exponential integrals. In the case of the coated wire, the formulation remained the same as the perfectly conducting case except that

the dielectric coating was replaced by a current sheet supporting an equivalent surface magnetic current. By comparison with measured and numerical data, it was observed that the derived expressions were highly accurate for short as well as long thin wires.

The finite length narrow groove was treated in a similar manner; in this case, an approximate boundary condition was enforced at the surface of the groove yielding an integral equation for the surface magnetic current which was then represented by the weighted sum of three travelling wave components. The agreement with reference data was reasonable and the small discrepancies were attributed to the approximate impedance boundary condition. To avoid use of the impedance boundary condition, one must resort to an exact eigenfunction representation of the fields within the cavity. Field continuity can then be applied at the aperture to obtain an integral equation for the surface magnetic current. To date, though, our attempts to obtain the 3×3 admittance matrix associated with this integral equation has yielded non-convergent mode sums, indicating that a non-conventional approach may be required to obtain convergent sums. One option may be to expand the physical basis in terms of subsectional roof-top basis functions to yield convergent mode sums for the fields inside the cavity.

7 Appendix

For a coated conducting wire in free space, Collin [30] gives the exact transcendental equation for the TM mode as

$$\frac{K_1(qb)}{pK_o(qb)} = \frac{\epsilon_r}{h} \frac{J_o(ha)Y_1(hb) - J_1(hb)Y_o(ha)}{J_o(hb)Y_o(ha) - J_o(ha)Y_o(hb)} \tag{38}$$

where ϵ_r is the complex permittivity of the coating, J_n is the Bessel function of the first kind of order n, Y_n is the Bessel function of the second kind of order n, K_n is the modified Bessel function of the second kind of order n and

$$\begin{aligned} q^2 &= \beta^2 - k_o^2 \\ h^2 &= \epsilon_r k_o^2 - \beta^2 \end{aligned}$$

in which β denotes the propagation constant of the reflected travelling waves.

For small t, the Bessel functions in (38) can be replaced by their small argument expansions [31] to obtain

$$\epsilon_r q^2 b \ln(.89qb) = -(\epsilon_r - 1)k_o^2(b-a) \tag{39}$$

which can be readily solved via an iterative approach such as the Newton-Raphson method.

8 References

1. J.H. VanVleck, F. Bloch, and M. Hamermesh, "Theory of radar reflection from wires or thin metallic strips", *J. Appl. Phys.*, Vol. 18, pp. 274-294, March 1947.

2. C.T. Tai, "Electromagnetic backscattering from cylindrical wires", *J. Appl. Phys.*, Vol. 23, pp. 1108-1205, 1952.

3. Y.Y. Hu, "Backscattering cross section of a center-loaded cylindrical antenna", *IEEE Trans. Antennas Propagat.*, Vol. AP-6, pp.140-148,1958.

4. E. Hallen, "Theoretical investigations into the transmitting and receiving quantities of antennae", *Nova Acta Regiae Societatis Scientiarum Upsaliensis*, Ser. IV, Vol. 11, No.4.

5. S.H. Dike and D.D. King, "The absorption gain and backscattering cross-section of the cylindrical antenna", *IEEE Trans. Antennas Propagat.* Vol. 40, pp.853-860; discussion in *IEEE Trans. Antennas Propagat.* Vol. 41, pp.926-934.

6. R.W.P. King, *The theory of linear antennas*, Harvard University Press, Cambridge, Massachusetts, 1956.

7. K. Lindroth, "Reflection of electromagnetic waves from thin metal strips", *Trans. Roy. Inst. Technol. Stockholm*, No. 91, 1955.

8. R.W.P. King and T.T. Wu, Chapter 4 in *The scattering and diffraction of waves*, Harvard University Press, Cambridge, Massachusetts, 1959.

9. R.W.P. King, "Current distribution in arbitrarily oriented receiving and scattering antenna", *IEEE Trans. Antennas Propagat.*, Vol. AP-20, pp. 152-159, March 1972.

10. R.W.P. King, A.W. Glisson, S. Govind, R.D. Nevels and J.O. Prewitt, "Currents and charges induced in an arbitrarily oriented electrically thin conductor with length upto one and one-half wavelengths in a plane wave field", *IEEE Trans. Electromagnetic Compat.*, Vol. EMC-19, pp.145-147, August 1977.

11. K.M. Chen, "Reactive loading of arbitrarily illuminated cylinders to minimize microwave backscattering", *Radio Sci.*, Vol. 69D, pp.1481-1502,

Nov. 1965.
12. E. Hallen, *Electromagnetic theory*, John Wiley and Sons, Inc., New York, 1962.
13. P. Ya. Ufimtsev, "Diffraction of plane electromagnetic waves by a thin cylindrical conductor",*Radio Eng. Electron.* 7, pp.241-249 (English translation of *Radiotekhn. i Elektron.* 7), 1962.
14. S. Hong, S. Borrison and D. Ford, "Short pulse scattering by a long wire", *IEEE Trans. Antennas Propagat.*, Vol. AP-16, pp. 338-342, May 1968.
15. O. Einarsson, Chapter 12 in *Electromagnetic and acoustic scattering by simple shapes*, ed. Bowman, Senior and Uslenghi, Hemisphere, New York, 1987.
16. O. Einarsson, "Electromagnetic scattering by a thin finite wire",*Acta Polytechnica Scandinavica*, Elec. Eng. Series, No. 23, Stockholm,1969.
17. L. Shen, "A simple theory of receiving and scattering antennas", *IEEE Trans. Antennas Propagat.*, pp.112-114, Jan. 1970.
18. L. Peters, Jr., "Endfire echo-area of long thin bodies", *IEEE Trans. Antennas Propagat.*, pp. 133-139, Jan. 1958.
19. L.A. Weinstein, *The theory of diffraction and the factorization method*, The Golem press, 1969.
20. C.L. Chen, "On the scattering of electromagnetic waves from a long wire", *Radio Sci.*, Vol. 3, pp. 585-597, June 1968.
21. T.T. Wu, "Theory of the dipole antenna and the two-wire transmission line", *Journ. of Math. Phys.*, Vol. 2, 1961.
22. J.H. Richmond, "Scattering by thin dielectric strips", *IEEE Trans. Antennas Propagat.*, Vol. AP-33, Jan. 1985.
23. T.B.A. Senior and J.L. Volakis, "Scattering by gaps and cracks", *IEEE Trans. Antennas Propagat.*, Vol. AP-37, pp.744-750, June 1989.
24. P.E. Mayes, "The equivalence of electric and magnetic sources", *IEEE Trans. Antennas Propagat.*, Vol. AP-6, pp.295-297, July 1958.
25. J.H. Richmond, "Green's function technique for near-zone scattering by cylindrical wires of finite conductivity", *IEEE Trans. Antennas Propagat.*, Vol. AP-28, pp.114-117,Nov. 1980.
26. J.M. Jin and J.L. Volakis, "A finite element-boundary integral formulation for three-dimensional cavity-backed apertures", *IEEE Trans. Antennas Propagat.*, Vol. AP-39, Jan. 1991.
27. C.H. Walter, *Travelling wave antennas*, pp.189-190, Dover, New York,

1970.
28. A.K. Dominek, H.T. Shamansky and N. Wang, "Scattering from three dimensional cracks", *IEEE Trans. Antennas Propagat.*, Vol. AP-37, May 1989.
29. K. Barkeshli and J.L. Volakis, "Electromagnetic scattering from an aperture formed by a rectangular cavity recessed in a ground plane", *J. of Electromag. Waves Appl.*, to appear in 1991.
30. R.E. Collin, *Field theory of guided waves*, pp.477-480, McGraw-Hill, New York, 1960.
31. G. Goubau, "Single conductor surface wave transmission line", *IEEE Trans. Antennas Propagat.*, Vol. 39, pp.619-624, June 1951.

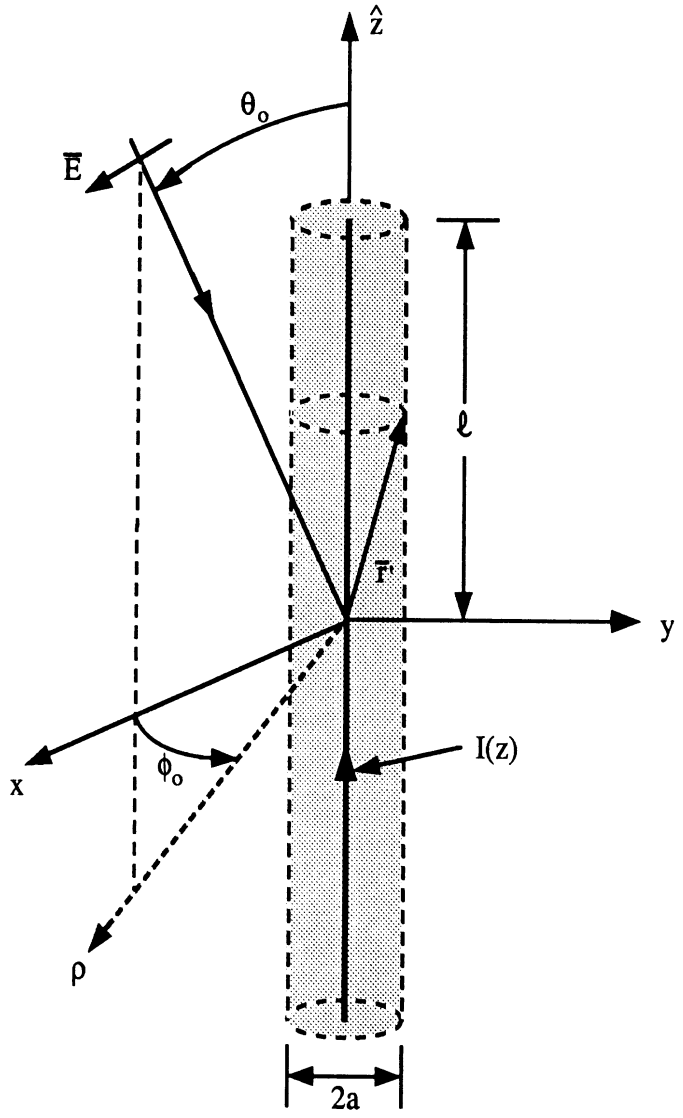

Figure 1. Wire geometry.

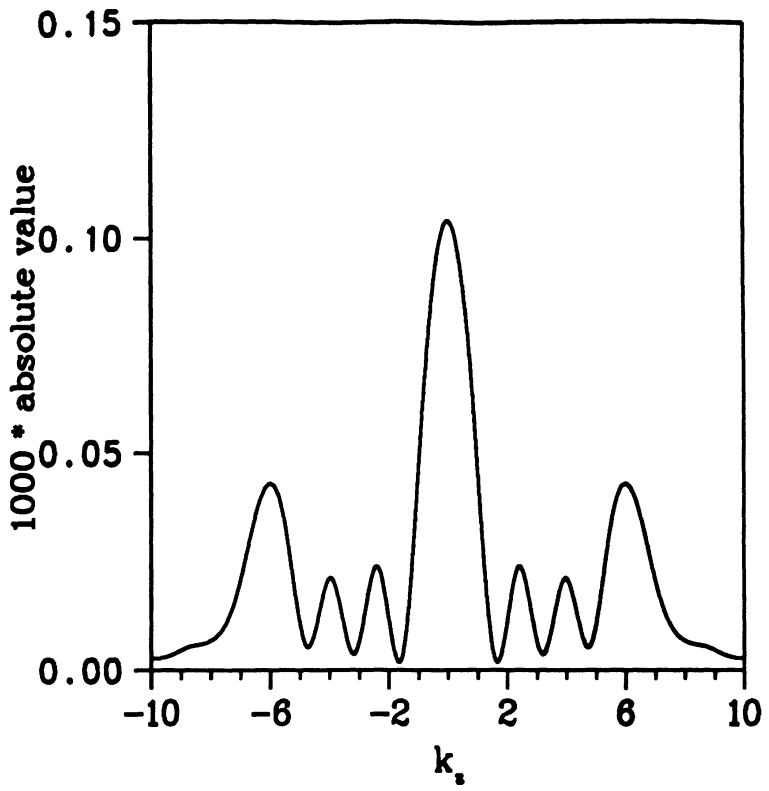

(a)

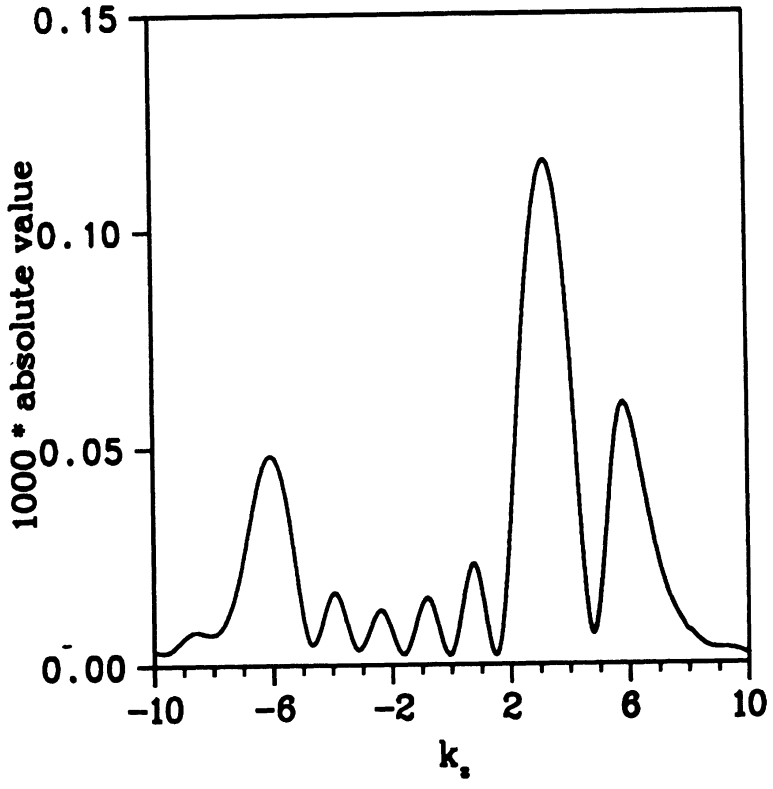

(b)

Figure 2: Current spectra for a 4λ wire of radius $.01\lambda$ at (a) normal incidence (b) oblique incidences ($\theta_o = 60°$)

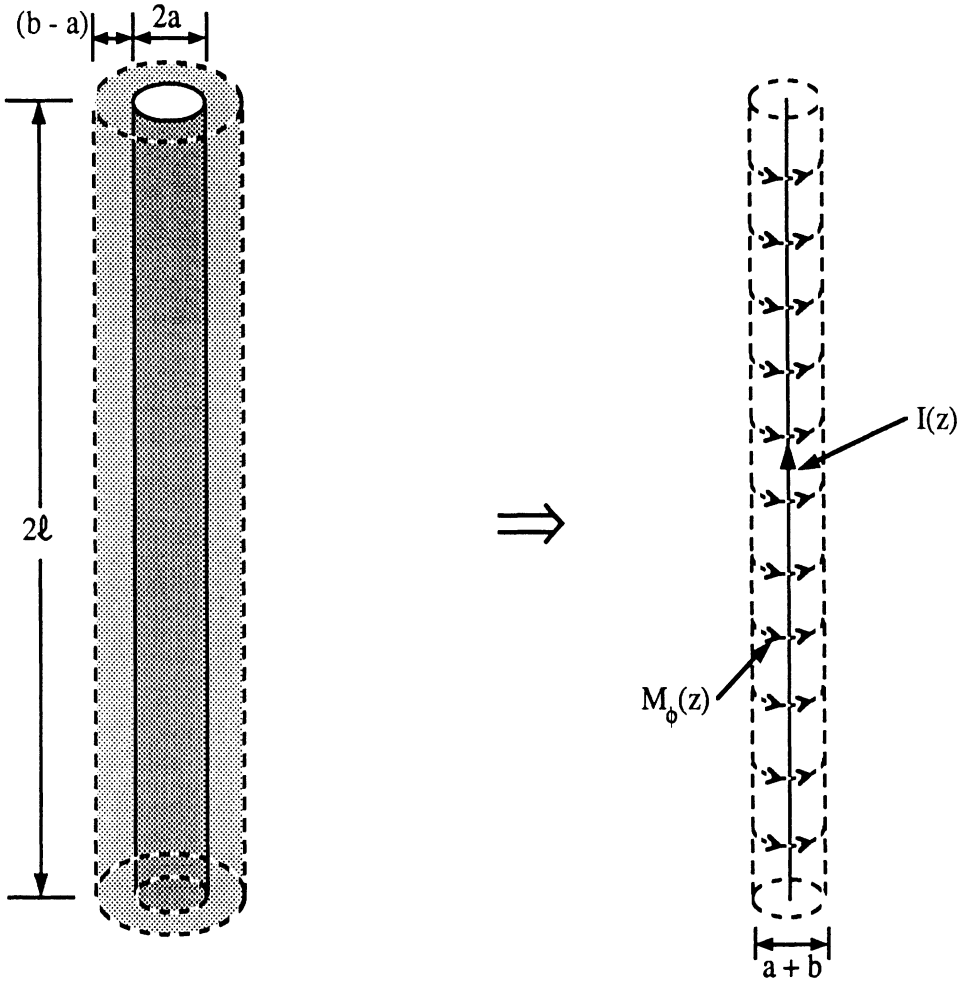

Figure 3. Illustration of the coated wire geometry and the proposed analytical model.

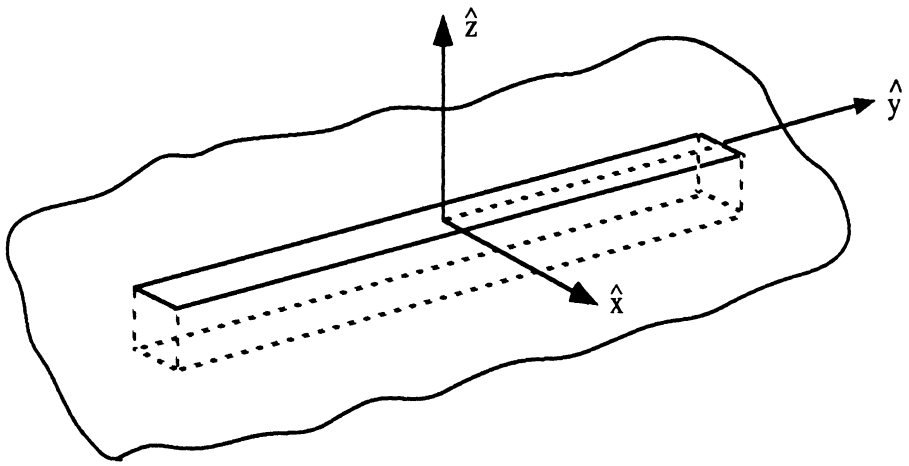

Figure 4: Geometry of finite length narrow rectangular groove.

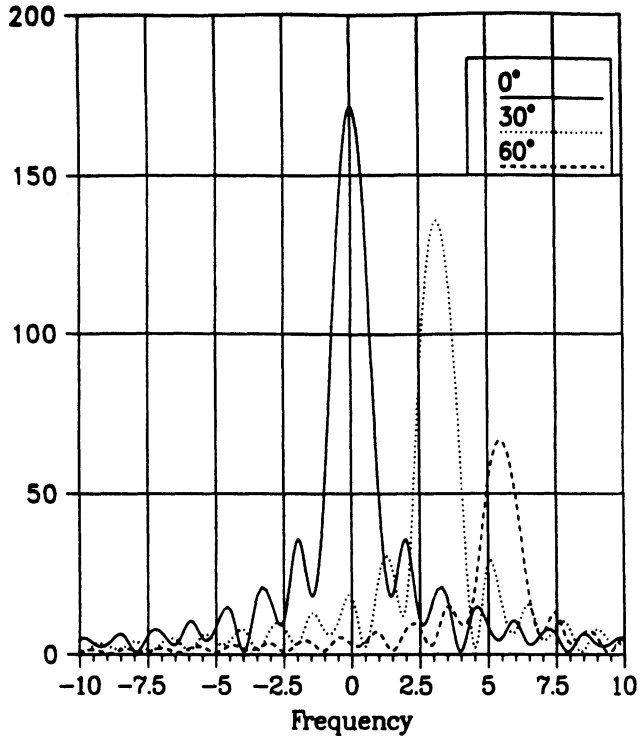

(a)

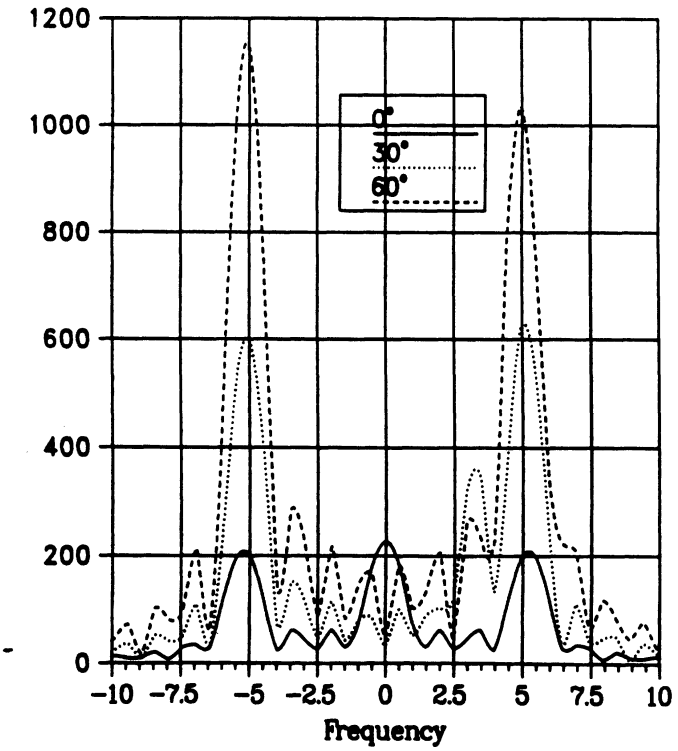

(b)

Figure 5: Current spectra for a 5λ long, $.05\lambda$ wide cavity with varying depths at normal and oblique incidences (a) cavity depth= $.1\lambda$ (b) cavity depth= $.4\lambda$

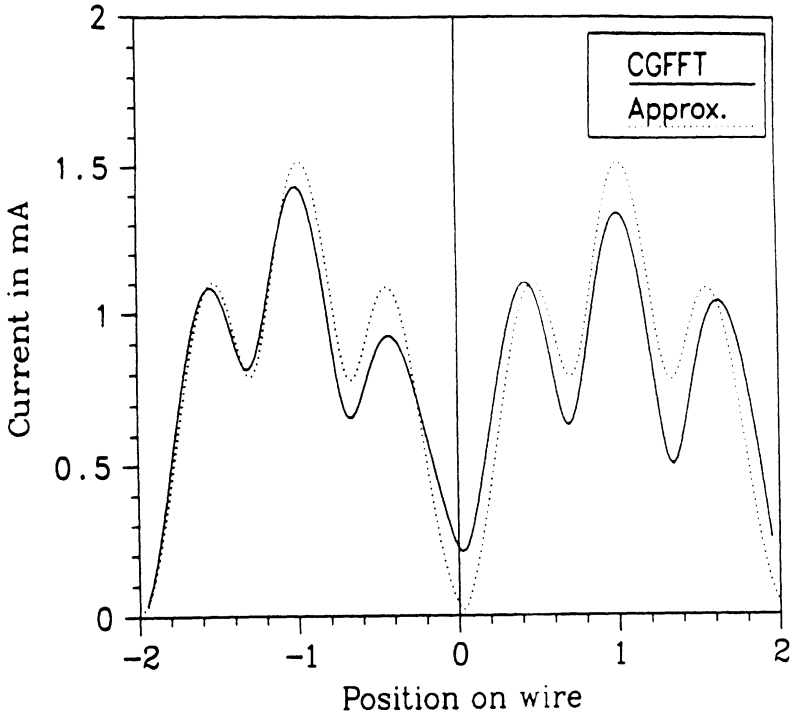

(a)

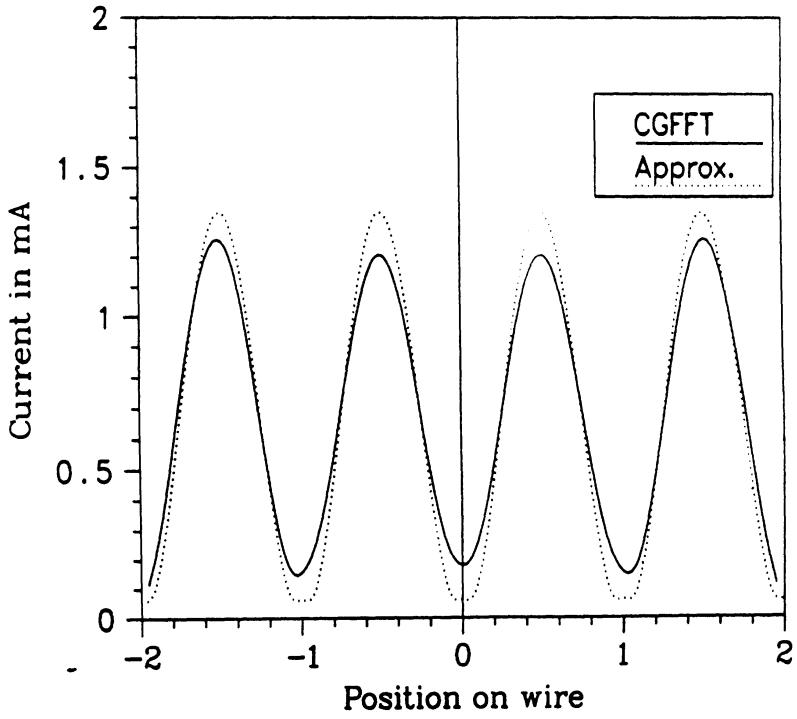

(b)

Figure 6: Current distribution for a 4λ wire having $a = .01\lambda$. Comparison of results obtained from the physical basis solution (dotted line) and from a CGFFT solution (solid line) of Pocklington's integral equation. (a)$\theta_o = 60°$, (b)$\theta_o = 90°$

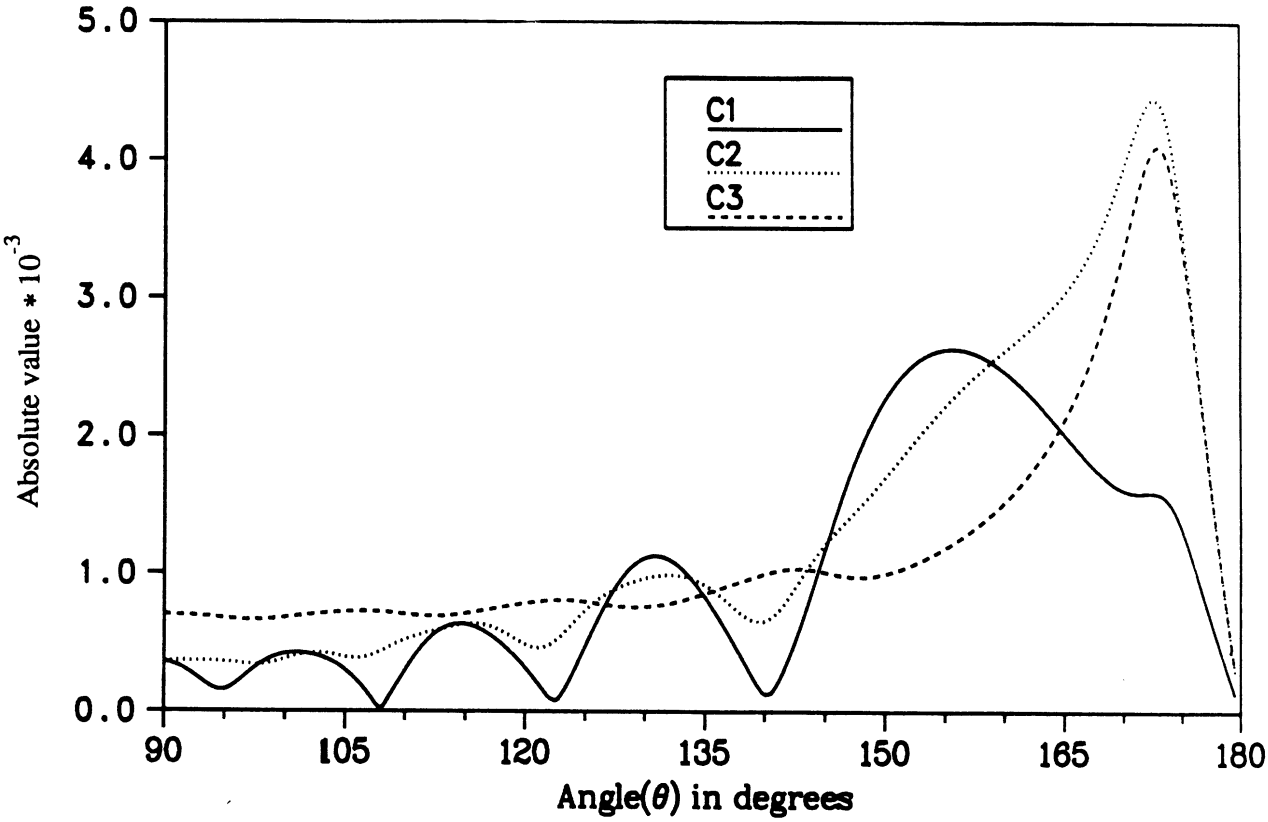

Figure 7: Travelling wave coefficients as a function of incidence angle for a 4λ wire having $a = .01\lambda$.

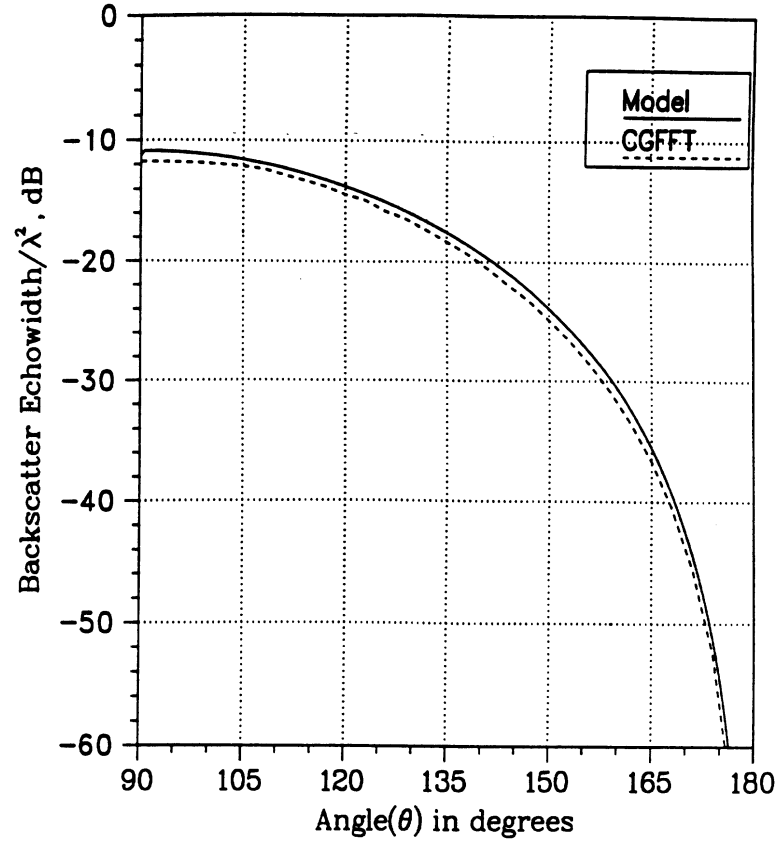

(a)

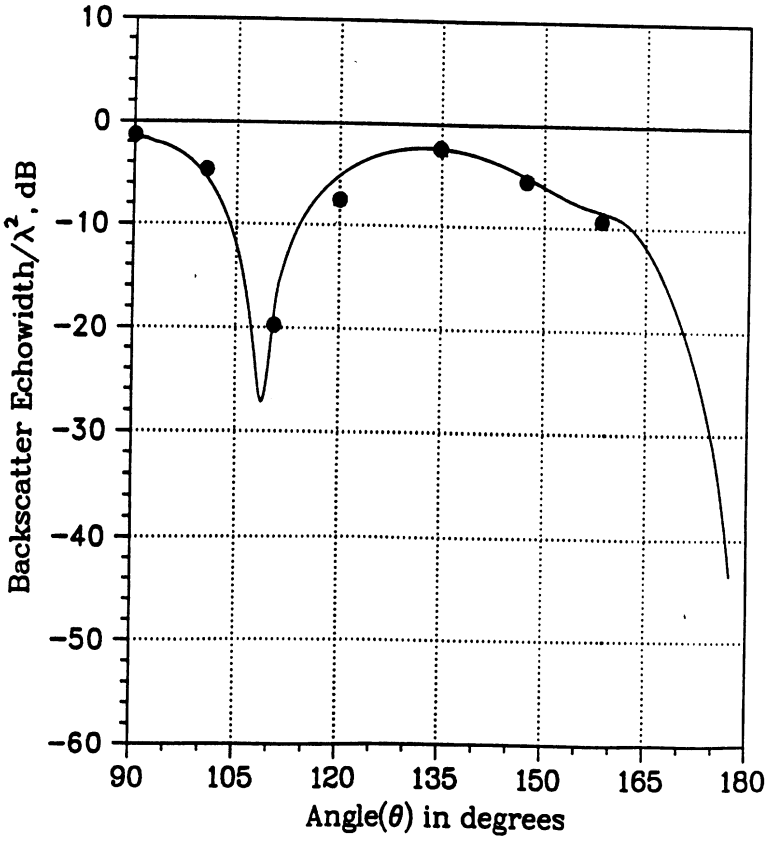

(b)

Figure 8: Backscatter patterns for wire having a radius of .05λ (a).25λ (b).1λ. Dots indicate measured data.

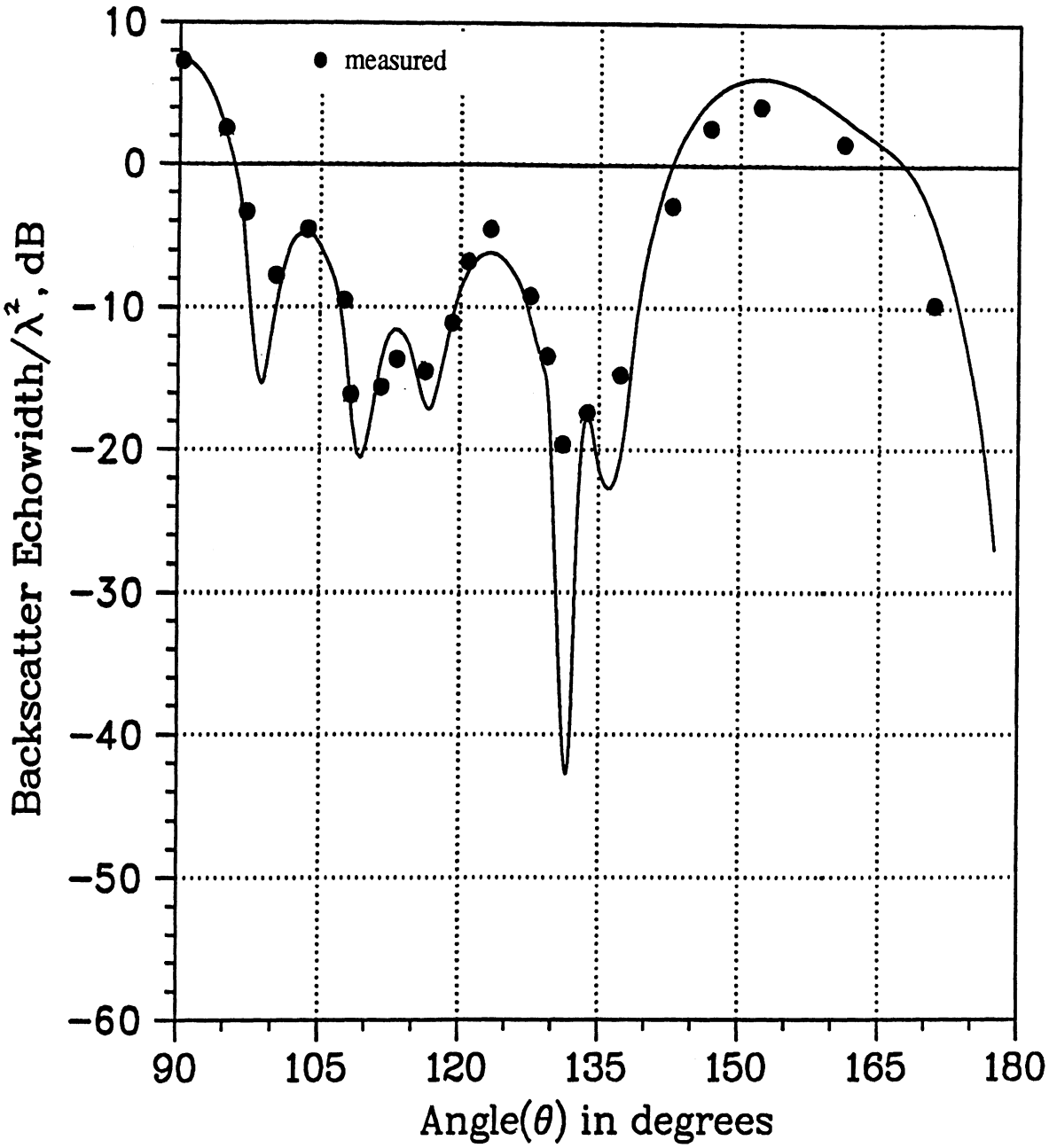

Figure 9: Backscatter pattern for a 3λ long wire of radius $.05\lambda$. Dots indicate measured data.

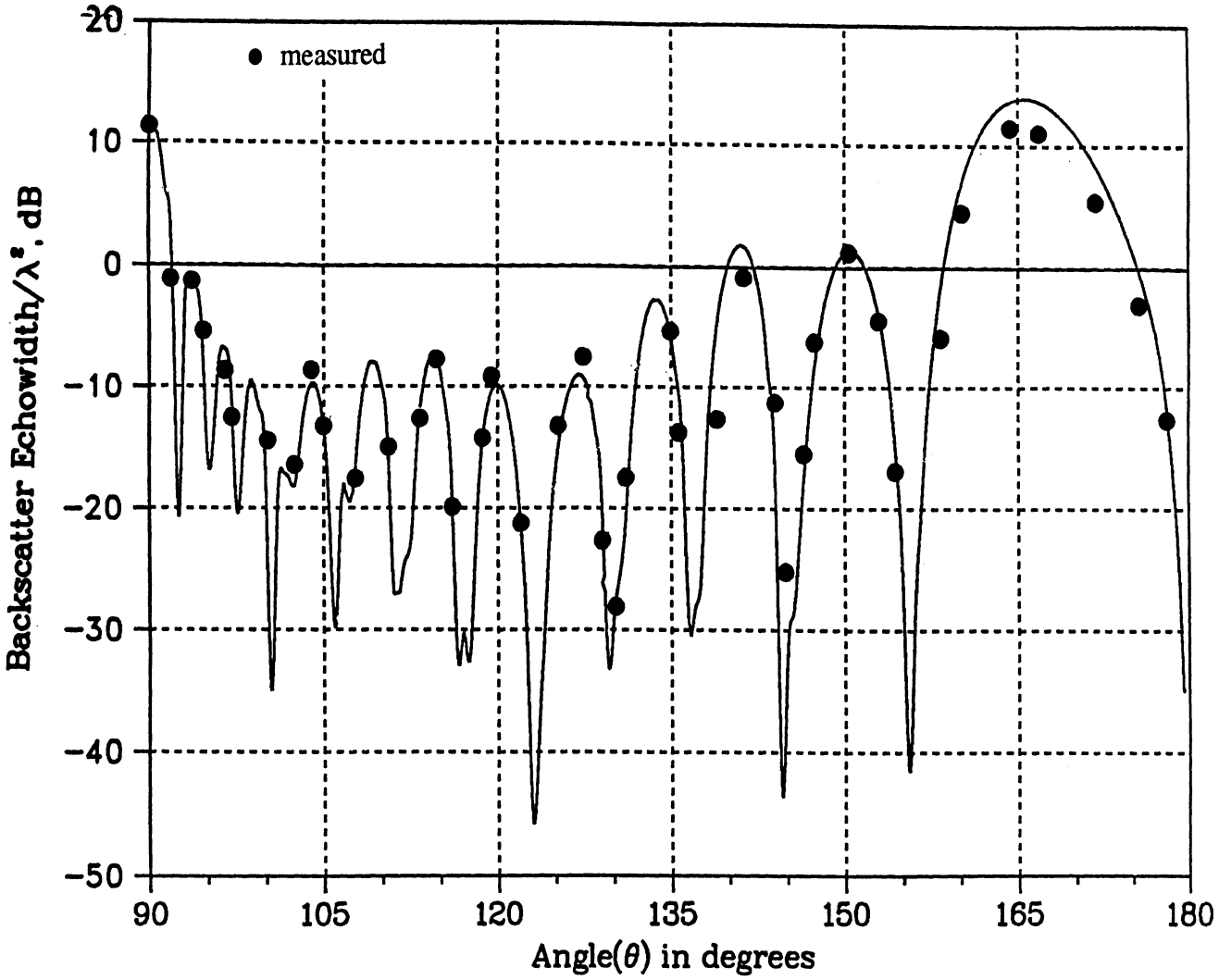

Figure 10: Backscatter pattern for a 11.05λ long wire having a radius .00147λ. Dots indicate measured data.

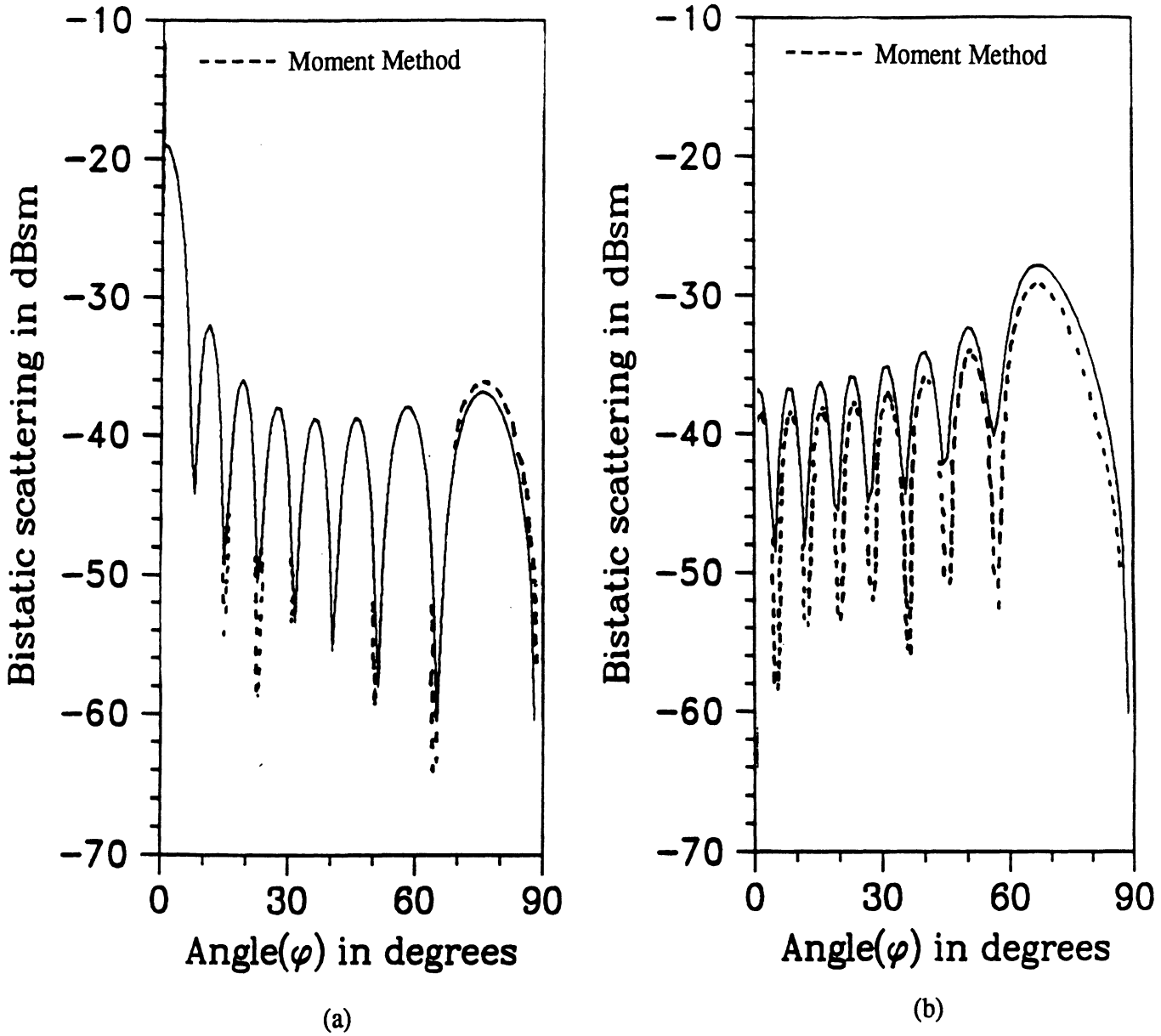

Figure 11: Bistatic pattern for a coated wire having $l = 8.33\lambda, \epsilon_r = 4, b = .0067\lambda, a = .0033\lambda$ (a)$\theta_o = 90^o$, (b)$\theta_o = 10^o$

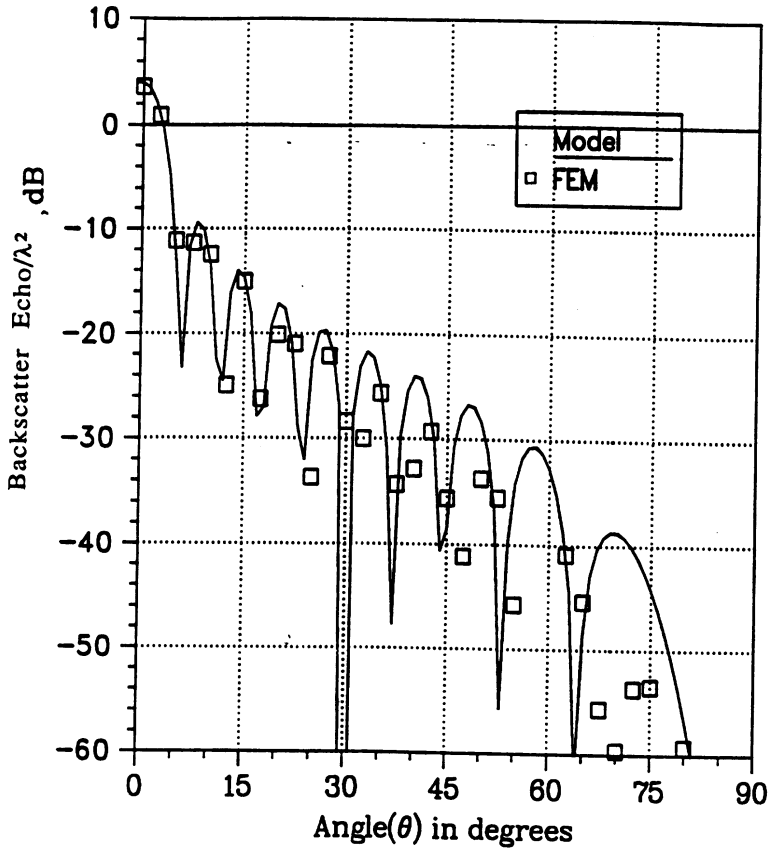

(a)

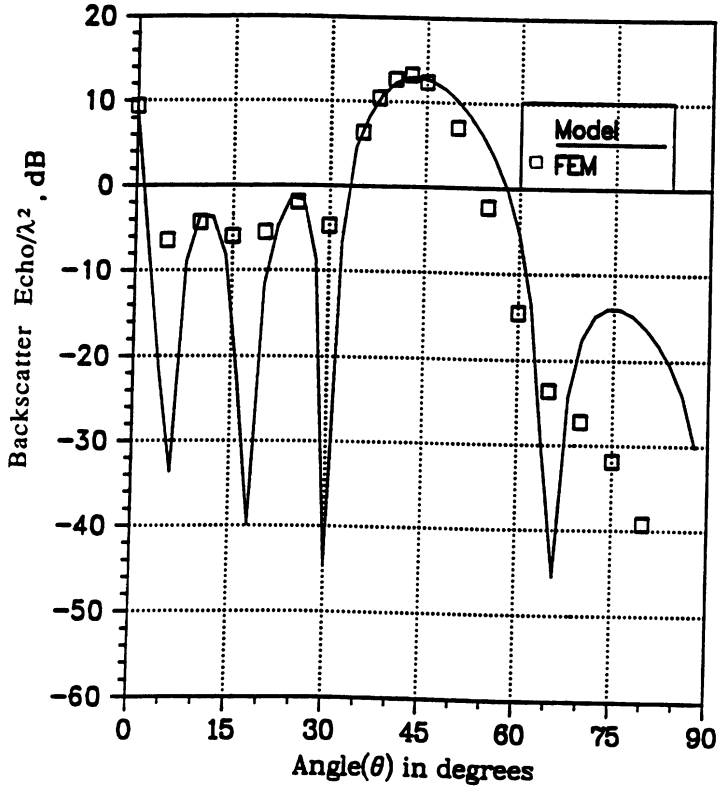

(b)

Figure 12: Backscatter pattern of a $5\lambda(2w = .05\lambda)$ long cavity for a depth of (a).1λ (b).3λ